Order in vertically aligned carbon nanotube arrays

H. Wang[a] and Z. Xu
Department of Materials Science and Engineering, Michigan Technological University, Houghton, Michigan 49931

G. Eres
Condensed Matter Sciences Division, Oak Ridge National Laboratory, Oak Ridge, Tennessee 37831

(Received 11 January 2006; accepted 6 April 2006; published online 24 May 2006)

We report the direct measurements on the bulk morphology of vertically aligned multiwalled carbon nanotube (CNT) arrays using small angle neutron scattering (SANS). SANS measurements at different heights of CNT arrays corresponding to different stages of the growth reveal increasing alignment order along the thickness and two distinctly different CNT morphologies. The observations suggest that the evolution of the macroscopic CNT morphologies be driven by competing collective growth and spatial constraints. © *2006 American Institute of Physics*.
[DOI: 10.1063/1.2206152]

Vertically aligned carbon nanotube (VACNT) arrays are ordered structures of CNTs (Refs. 1–3) that can exploit the remarkable properties of individual nanotubes in macroscopic applications.[4–6] Alignment is an important parameter for characterizing CNT bulk assemblies in terms of the theoretical limits of electrical and thermal conductivities and mechanical strength for individual CNTs. Here we report the direct measurements of the degree of order in as-grown vertically aligned multiwalled CNT arrays using small angle neutron scattering. The scattering patterns reveal continuously varying alignment order along the growth direction and two distinctly different morphologies of CNTs. Although the measurements were performed on multiwalled CNTs, the method described in this letter is also applicable to aligned single-wall CNTs and nanowires.

Small angle neutron scattering (SANS) has recently been employed to characterize the dispersion of CNTs in surfactant solutions.[7,8] Here we describe the use of SANS to measure the order and alignment in VACNT arrays. Vertically aligned multiwalled CNTs were grown by chemical vapor deposition on a Si (100) wafer using a two-layer metal catalyst film consisting of 10 nm of Al and 1 nm of Fe. The feedstock for the CNT growth is 9 SCCM (SCCM denotes cubic centimeter per minute at STP) of acetylene, 100 SCCM of hydrogen, 250 SCCM of helium, and 4 mg/h of thermally evaporated ferrocene, $Fe(C_5H_5)_2$. Ferrocene enhances the efficiency of the predeposited catalyst film and postpones growth termination, resulting in higher CNT growth rates and thicker CNT films.[3] The CNT mat shown in Fig. 1(a) has lateral dimensions of 25×25 mm^2 and uniform thickness of 4.5 mm. In this study two samples were measured, the entire sample aforementioned and a 1 mm wide Si strip cleaved from the parent sample with aligned CNTs intact.

SANS experiments were performed at the NIST Center for Neutron Research on the NG7 30 m SANS instrument. Three different instrumental configurations yield a wide Q range of 0.0008–0.4 Å^{-1}. In the measurement geometry shown in Fig. 1(b) the neutron beam is incident on the side of CNT mat perpendicular to the growth direction. The beam footprint of $1/32\times1/4$ in.^{2}, represented by the red rectangles, is scanned from the substrate to the top of the CNT forest. The two-dimensional (2D) scattering data were corrected for background and detector efficiency and azimuthally averaged to yield the scattering cross section at $Q=0.01$ Å^{-1}.

The 2D scattering patterns for the large sample are shown in Figs. 1(c)–1(f). The intensity is anisotropic, enhanced along the Y and suppressed along the X coordinate, and indicates vertical (horizontal in the scattering measurement) alignment of CNTs. The pattern anisotropy becomes more prominent as the height from the substrate h increases, indicating that the alignment is improving. Figure 1(g) shows the azimuthal plot at $Q=0.01$ Å^{-1}. The angular profiles are fitted with single Lorentz functions. The solid lines through symbols are the best fit.

The enhanced alignment is characterized by the Lorentzian width, which is plotted in Fig. 1(h) (red symbols). The Lorentzian width decreases linearly with h before leveling off, indicating narrowing of the angular dispersion of CNTs from the substrate normal. The degree of the alignment can also be described by a nematic order parameter using Hermans's orientation function. The resulting order parameter, f, has limiting values of 0 and 1, corresponding to random orientation and perfect alignment, respectively. Figure 1(h) shows that the order parameter (blue symbols) increases linearly with h.

The 1 mm thick sample provides more details of the morphology of the aligned tubes. Figures 2(a)–2(f) show 2D scattering patterns of CNT, which, in addition to demonstrating the general feature of improving alignment with h, also reveal structures other than aligned tubes [Figs. 2(a)–2(c)]. Scanning electron microscopy images illustrating the real space morphologies are shown in Figs. 2(g)–2(k). While Fig. 2(g) shows dominantly helical and zigzag morphology close to the substrate,[9] there also exist regions with straight tubes at the same height. The coexistence of the two morphologies of tubes, one growing relatively straight whereas the other taking regular zigzag or helical path, becomes evident in Fig. 2(h). The interplay of the two morphologies is responsible for the broadening of the scattering pattern shown in Figs. 2(a)–2(f).

[a]Electronic mail: wangh@mtu.edu

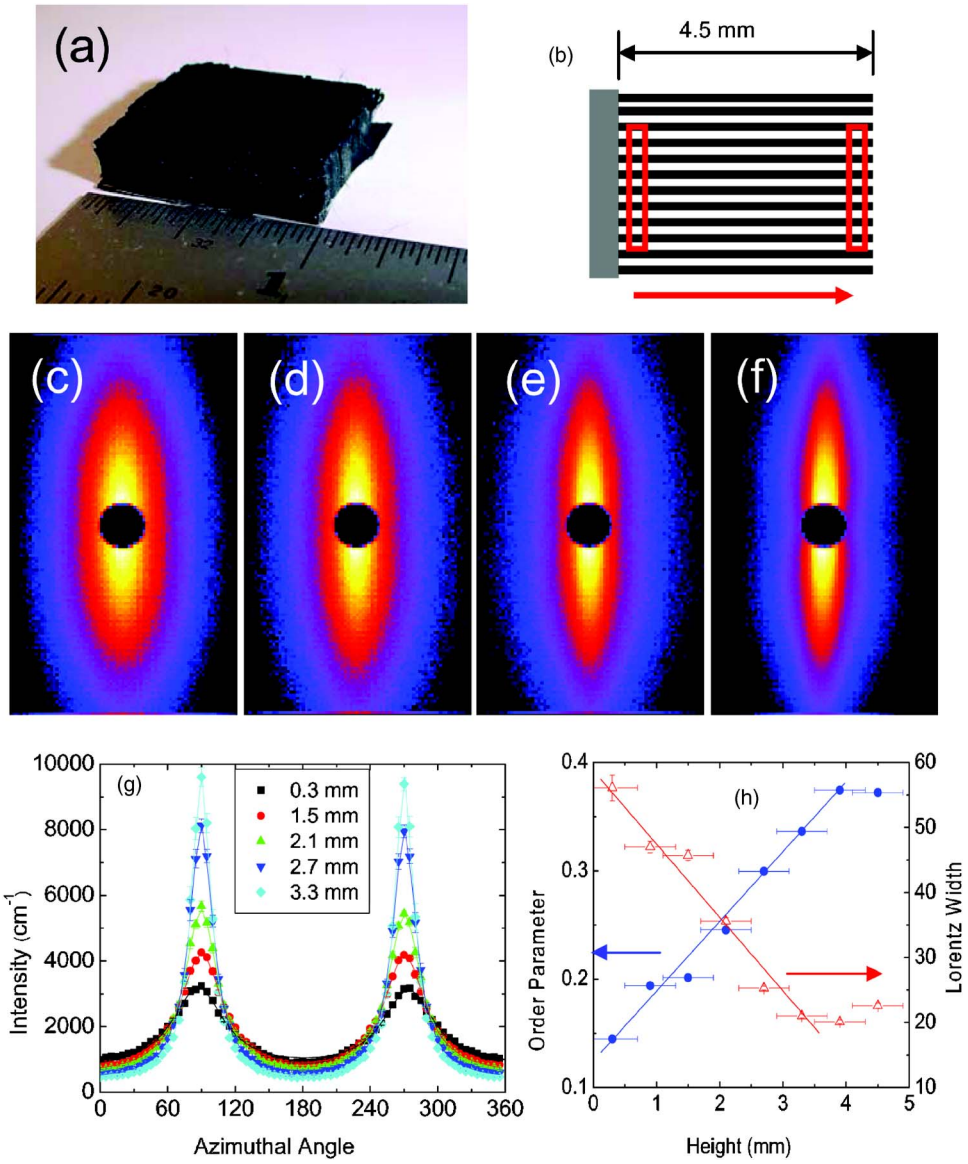

FIG. 1. (Color online) (a) A photograph of the $25\times25\times4.5$ mm^3 CNT sample in this study. (b) The schematics of the scattering geometry show the neutron beam incident perpendicular to the substrate normal. The red rectangles represent the beam footprint of $1/32\times1/4$ in.^{2}. [(c)–(f)] 2D scattering patterns at 0.9, 2.1, 2.7, and 3.9 mm from the substrate, respectively. The anisotropy indicates the alignment of CNTs perpendicular to the substrate. (g) Azimuthal plot at $Q=0.01$ Å^{-1} for several measurement positions from the substrate. The solid lines through the symbols are the best fit with Lorentz functions. (h) The Lorentzian width (red symbols) and the nematic order parameter (blue symbols) are shown as functions of the distance from the substrate. The narrowing of the Lorentzian width and the increase of the order parameter both indicate that the alignment of CNTs improves with increasing distance from the substrate.

The azimuthal plot at $Q=0.01$ Å^{-1} [Fig. 2(l)] shows that the profiles near the substrate display two superimposed peaks, with a narrow peak corresponding to the straight tubes and a broad peak corresponding to the zigzag tubes. The narrow peak remains relatively constant, but the broad peak narrows with h. A two-peak model with a Lorentzian function for the narrow peak and a Gaussian for the broad peak was used to fit the data. The best model fit [solid lines in Fig. 2(l)] indicates that the Lorentzian width of the narrow peak remains constant at $17°\pm3°$, whereas the Gaussian full width at half maximum decreases linearly with h [Fig. 2(m)].

The data are consistent with a root growth mechanism as illustrated schematically in Fig. 2(n). During the early stage, CNTs grow freely over the entire substrate. Since the density of the catalyst particles is high, simultaneous growth of CNTs results in vertical alignment that is induced by crowding. With progression of growth the interaction among the tubes increases. The average speed of the advancing growth front suppresses the fast growing CNTs and stresses them to grow into curved structures, resulting in poorer macroscopic ordering of the alignment. At the late stage, the mat is thick and the growth heterogeneity occurs over large lateral scales. In regions where most tubes are growing faster than the average, the capping stress forces CNTs to grow collectively into a helical or zigzag morphology, further degrading the overall alignment of tubes.

In summary, we describe the direct measurements of the bulk morphology of VACNT arrays using SANS. SANS measurements at different heights corresponding to different stages of the growth reveal increasing alignment order along the thickness and two distinctly different CNT morphologies. We argue that the evolution of the macroscopic CNT morphologies is driven by the competing factors of collective growth and spatial constraints. We demonstrate the use of neutron scattering as a general method for characterizing the order, the alignment, and the homogeneity of macroscopic nanostructure assemblies, which are important for understanding the fundamental mechanisms of nanomaterial synthesis and their assembly into bulk structures for applications.

One of the authors (H.W.) acknowledges the NSF Career Award DMR-0348895 and the support of the National Institute of Standards and Technology in providing the neutron research facilities used in this work. Another author (G.E.) is supported by the Oak Ridge National Laboratory, managed by UT-Battelle, LLC, for the U.S. Department of Energy under Contract No. DE-AC05-00OR22725 and the

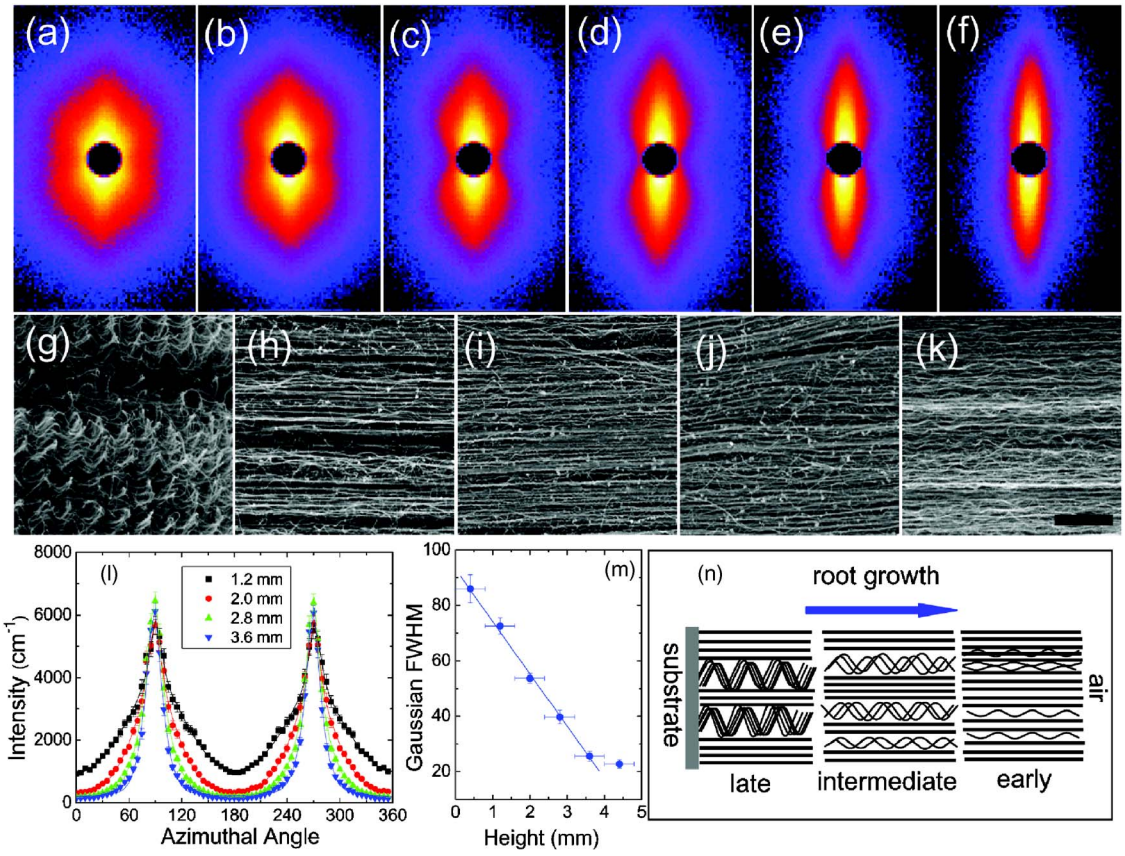

FIG. 2. (Color online) [(a)–(f)] 2D SANS scattering patterns of the aligned CNTs at 0.4, 1.2, 2.0, 2.8, 3.6, and 4.4 mm from the 1 mm thick sample, respectively. [(g)–(k)] SEM images of CNT morphology near the substrate and at 1, 2, 3, and 4 mm from the substrate. The scale bar in (k) is 2 μm and is the same for all images. (l) Azimuthal plot of selected SANS patterns at Q=0.01 Å^{-1}. The solid lines through symbols are the best fit with superimposed Lorentz and Gauss functions. (m) The Gaussian FWHM decreases linearly with the distance from the substrate. (n) A schematic of the root growth mechanism illustrates that the initially straight CNTs develop curved morphologies in latter stages of growth.

Laboratory-Directed Research and Development Program at ORNL. Part of this research was conducted at the Center for Nanophase Materials Sciences, which is sponsored at Oak Ridge National Laboratory by the Division of Scientific User Facilities, U.S. Department of Energy.

[1]Z. F. Ren, Z. P. Huang, J. W. Xu, J. H. Wang, P. Bush, M. P. Siegal, and P. N. Provincio, Science **282**, 1105 (1998).
[2]Z. W. Pan, S. S. Xie, B. H. Chang, C. Y. Wang, L. Lu, W. Liu, W. Y. Zhou, W. Z. Li, and L. X. Qian, Nature (London) **394**, 631 (1998).
[3]G. Eres, A. A. Puretzky, D. B. Geohegan, and H. Cui, Appl. Phys. Lett. **84**, 1759 (2004).
[4]W. A. de Heer, A. Châtelain, and D. Ugarte, Science **270**, 1179 (1995).
[5]Y. H. Lin, F. Lu, Y. Tu, and Z. F. Ren, Nano Lett. **4**, 191 (2004).
[6]A. B. Dalton, S. Collins, E. Munoz, J. M. Razal, V. H. Ebron, J. P. Ferraris, J. N. Coleman, B. G. Kim, and R. H. Baughman, Nature (London) **423**, 703 (2003).
[7]H. Wang, W. Zhou, D. L. Ho, K. I. Winey, J. E. Fischer, C. J. Glinka, and E. K. Hobbie, Nano Lett. **4**, 1789 (2004).
[8]K. Yurekli, C. A. Michell, and R. Krishnamoorti, J. Am. Chem. Soc. **126**, 9902 (2004).
[9]V. Bajpai, L. M. Dai, and T. Ohashi, J. Am. Chem. Soc. **126**, 5070 (2004).